Journal of Statistical Physics, Vol. 60, Nos. 3/4, 1990

Exact Coexistence Surfaces Containing Double Critical Points for a Three-Component Solution on the Bethe, Honeycomb, and Square Lattices

Dale A. Huckaby[1] **and Masato Shinmi**[1]

Received August 2, 1989; final February 21, 1990

A model is considered in which the bonds of a lattice are covered by rodlike molecules. Neighboring molecular ends interact with orientation-dependent interactions. The model exhibits closed -loop phase diagrams and double critical points. Exact coexistence surfaces are calculated for the model on the Bethe, honeycomb, and square lattices. The nature of the doubling of the critical exponent β near a double critical point is calculated. The behavior of the critical line in the neighborhood of a double critical point is calculated exactly.

KEY WORDS: Ising model; phase transitions; double critical point; three-component.

1. INTRODUCTION

Double critical points, points at which two critical points coalesce, have been extensively studied using lattice models of binary solutions.[1-6] We recently introduced an exactly solvable lattice model of a ternary solution which exhibits a double critical point.[7] The model contains molecules of types AA, BB, and AB. A hydrogen bond can form between neighboring unlike molecular ends. At a small, constant mole fraction X_{AB} of the amphiphile AB, a closed loop occurs with upper and lower critical solution points at the temperatures T_U and T_L. As the mole fraction of the amphiphile increases, the closed loop shrinks to a double critical point at X_{AB}^D and T_D.

In Section 2 we generalize the model so as to include hydrogen bonds between two type A molecular ends. In Section 3 we calculate exact closed-loop phase diagrams for both the original and the generalized model on the

[1] Department of Chemistry, Texas Christian University, Fort Worth, Texas 76129.

0022-4715/90/0800-0347$06.00/0

Bethe, honeycomb, and square lattices. In the generalized version an additional miscibility gap can occur which has an upper critical point at a temperature which is below that of the lower critical point of the closed loop. These two critical points can coalesce to give a second double critical point.

As discussed by several authors,[1–11] at a double critical point the critical exponents have double their normal values. In Section 4 we consider the nature of the doubling of the exponent β. The difference in the mole fractions of AA and BB molecules is the order parameter associated with β in the model. We were unable to observe the doubling of β in $X_{AA}-X_{BB}$, T planes at constant X_{AB} near the double critical point at which the upper and lower critical points on the closed loop coalesce. Of course, the closed loop shrinks to a point at this type of double critical point. However, the doubling of the exponent β is clearly seen in a constant-X_{AB} plane at the double critical point which occurs in the generalized model when the lower critical point of the closed loop coincides with the upper critical point of the low-temperature miscibility gap.

In Section 5 we give exact expressions for the line of critical points for the model on the Bethe, honeycomb, and square lattices, and we show that for each of these lattices the critical line in the neighborhood of the double critical point, which occurs as the closed loops shrink to a point, behaves as

$$\begin{aligned}(T_U-T_L)/2T_D &\sim A(X_{AB}^D-X_{AB})^{1/2}\\ (T_U+T_L)/2T_D &\sim 1+B(X_{AB}^D-X_{AB})\end{aligned} \tag{1}$$

Exact expressions are obtained for the lattice-dependent constants A and B for each of the three lattices. The behavior given by Eq. (1) is similar to the behavior which has been found experimentally for some ternary systems.[8–10]

2. THE GENERALIZED MODEL

We consider a model in which rodlike molecules of types AA, BB, and AB occupy the bonds of a lattice. Each portion of a type A (type B) molecular end which faces a neighboring molecular end can be in any one of q_A (q_B) different states, only one of which can form a bond with a neighboring molecular end. A type A molecular end forms a hydrogen bond with energy δ_{AB} (or δ_{AA}) with a neighboring type B (or type A) molecular end if both see each other as being in bonding states; otherwise, molecular ends interact with energies ε_{AB}, ε_{AA}, or ε_{BB}. This is a generalization of the model previously studied[7] in which hydrogen bonds formed only between *unlike* molecular ends; i.e., $\delta_{AA}=\varepsilon_{AA}$. Configurations of

molecules in the model on the Bethe, honeycomb, and square lattices are illustrated in Fig. 1.

If we connect all neighboring molecular ends with links, every vertex in the resulting graph Λ can be considered to be covered by two graphs, a graph g_2 with a link joining the two molecular ends of a single molecule and a graph g_r with links connecting neighboring ends, each from a different molecule. (If every pair of vertices in g_r is connected, Λ is called a line graph.)

The grand canonical partition function is given as

$$\begin{aligned}\Xi = \sum & \left[(q_A q_B - 1)\, e^{-\varepsilon_{AB}/kT} + e^{-\delta_{AB}/kT}\right]^{N_{AB}^{(r)}} \\ & \times \left[(q_A^2 - 1)\, e^{-\varepsilon_{AA}/kT} + e^{-\delta_{AA}/kT}\right]^{N_{AA}^{(r)}} (q_B^2 e^{-\varepsilon_{BB}/kT})^{N_{BB}^{(r)}} \\ & \times (e^{\mu_{AB}/kT})^{N_{AB}^{(2)}} (e^{\mu_{AA}/kT})^{N_{AA}^{(2)}} (e^{\mu_{BB}/kT})^{N_{BB}^{(2)}} \end{aligned} \tag{2}$$

where $N_{AB}^{(j)}$, $N_{AA}^{(j)}$, and $N_{BB}^{(j)}$ are the number of neighboring pairs of AB, AA, and BB ends on g_j graphs.

Since vacant sites are not allowed, the chemical potentials μ_{AB}, μ_{AA}, and μ_{BB} all tend to infinity; however, differences such as $\mu_{AB} - \mu_{AA}$ or $\mu_{AB} - \mu_{BB}$ are finite variables. The sum in Eq. (2) is over all configurations, where a specification of the molecular ends A and B defines a configuration in the sum.

If N_A is the number of type A ends, N_B is the number of type B ends, and $N = N_A + N_B$, then

$$\begin{aligned} N_{AA}^{(j)} &= [(j-1)\, N_A - N_{AB}^{(j)}]/2 \\ N_{BB}^{(j)} &= [(j-1)(N - N_A) - N_{AB}^{(j)}]/2 \end{aligned} \tag{3}$$

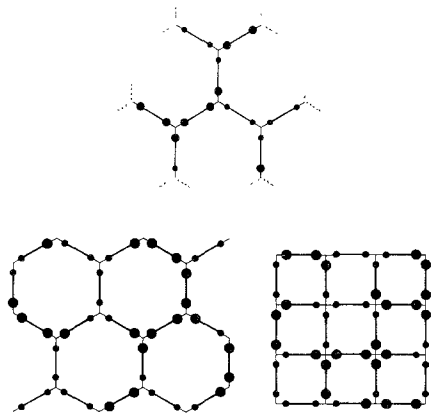

Fig. 1. Molecular configurations on the Bethe lattice, the honeycomb lattice, and the square lattice. Molecular ends of type A and B are represented by balls of two different sizes.

The grand canonical partition function, except for a constant factor, can then be written as

$$\Xi = \sum (e^{-2R})^{N_{AB}^{(r)}} (e^{-2L})^{N_{AB}^{(2)}} (e^{2h})^{N_A} \tag{4}$$

where

$$e^{-2R} = \frac{(1-\sigma_{AB})\, e^{-\gamma/kT} + \sigma_{AB} e^{-\varepsilon/kT}}{[(1-\sigma_{AA}) + \sigma_{AA} e^{-\delta/kT}]^{1/2}} \tag{5}$$

$$L = (\mu_{AA} + \mu_{BB} - 2\mu_{AB})/4kT \tag{6}$$

$$e^{2h} = (q_A/q_B)^{r-1} [(1-\sigma_{AA}) + \sigma_{AA} e^{-\delta/kT}]^{(r-1)/2} \times \exp\{-[(r-1)(\varepsilon_{AA} - \varepsilon_{BB}) - (\mu_{AA} - \mu_{BB})]/2kT\} \tag{7}$$

Here $\gamma = \varepsilon_{AB} - (\varepsilon_{AA} + \varepsilon_{BB})/2$, $\varepsilon = \delta_{AB} - (\varepsilon_{AA} + \varepsilon_{BB})/2$, and $\delta = \delta_{AA} - \varepsilon_{AA}$, and $\sigma_{AB} = 1/(q_A q_B)$ and $\sigma_{AA} = 1/q_A^2$ are temperature-independent "cross sections" for bond formation.

If we let $S_i = +1$ ($S_i = -1$) indicate that a site $i \in \Lambda$ is covered by a type A (type B) end, then Eq. (4) implies that the model is equivalent to a spin-1/2 Ising model on Λ which has a coupling constant L between the spins on each g_2 graph, a coupling constant R between interacting spins on each g_r graph, and a field h at each vertex of Λ.

3. PHASE DIAGRAMS WITH DOUBLE CRITICAL POINTS

The mole fractions of AA, BB, and AB molecules in the model are given by the equations

$$\begin{aligned} X_{AA} + X_{BB} + X_{AB} &= 1 \\ |X_{AA} - X_{BB}| &= I_\Lambda \\ X_{AB} &= (1-\sigma_\Lambda)/2 \end{aligned} \tag{8}$$

where $I_\Lambda = |\langle S_i \rangle_{i \in \Lambda}|$ is the magnetization and $\sigma_\Lambda = \langle S_i S_j \rangle_{i,j \subset g_2}$ is a correlation function for the Ising model on the associated lattice Λ.[12-14]

For the case $R > 0$ and $L > 0$, corresponding to a ferromagnetic Ising model, $h = 0$ is a necessary condition for phase separation into AA-rich and BB-rich phases. The relationships between L_c and R_c along the line of critical points have been calculated exactly for the model on the Bethe, honeycomb, and square lattices.[12-14] These relationships are

$$\begin{aligned} e^{-2L_c} &= (e^{4R_c} - 5)/(3e^{4R_c} + 1) && \text{Bethe} \\ \coth L_c &= \sqrt{3}\,(e^{4R_c} - 1)/(e^{4R_c} + 3) && \text{honeycomb} \\ e^{-2L_c} &= -1 + \sqrt{2} \tanh 2R_c && \text{square} \end{aligned} \tag{9}$$

For a given R_c, phase separation occurs if $L > L_c$. [As is apparent from Eqs. (4) – (6), R is constant at constant T, and increasing L at constant R corresponds to decreasing the mole fraction of AB molecules, thus enhancing the separation.] The minimum value of R_c for separation, which is calculated by letting $L_c \to \infty$ in Eq. (9), is given for each of the lattices as

$$\begin{aligned} &\min R_c = (\ln 5)/4 = 0.402 && \text{Bethe} \\ &\min R_c = [\ln(3+2\sqrt{3})]/4 = 0.467 && \text{honeycomb} \\ &\min R_c = [\ln(3+2\sqrt{2})]/4 = 0.441 && \text{square} \end{aligned} \tag{10}$$

For the case $R > 0$, $L > 0$, and $h = 0$, closed-form expressions for I_A and σ_A as functions of R and L have been calculated for each of the three lattices.[12–14] These expressions, given in the Appendix, can be inserted into Eq. (8) to obtain the entire coexistence surface in temperature–composition space in terms of the parameters R and L.

The intersection of the coexistence surface with a constant-X_{AB} plane, which gives the closed-loop phase diagram in the $X_{AA} - X_{BB}$, T plane, is calculated as follows. We define the reduced parameters $T' = 2kT/\gamma$, $s = -\varepsilon/\gamma$, and $u = -\delta/\gamma$. The parameters s and u are fixed for a given system. For a given T', we calculate R_c from Eq. (5), and then calculate L_c from Eq. (9). These values of R_c and L_c, together with the closed-form expression for σ_A, are then used to obtain $X^c_{AB}(R_c, L_c)$. This gives the point T'_c and $X_{AA} = X_{BB}$ on the coexistence curve in the $X_{AA} - X_{BB}$, T' plane which has this constant value of X_{AB}. The following procedure is used to calculate other points on the coexistence curve in this plane. A temperature T'_1 is chosen and used to calculate a value R_1. The parameter L is then increased from L_c until a value L_1 is found which satisfies $X_{AB}(R_1, L_1) = X^c_{AB}(R_c, L_c)$. The temperature T'_1 and the equation $|X_{AA} - X_{BB}| = I_A(R_1, L_1)$ give the coordinates of a symmetric pair of points on the coexistence curve in the $X_{AA} - X_{BB}$, T' plane which has this constant value of X_{AB}.

We calculated several closed-loop phase diagrams for the Bethe, honeycomb, and square lattices for the case $q_A = q_B = 6$, $s = 1$, and $u = 0$. The case $u = 0$ corresponds to the original model of ref. 7 in which hydrogen bonding occurs only between unlike molecular ends. The phase diagram for the honeycomb lattice is illustrated in Fig. 2, and the phase diagram for the square lattice is illustrated in Fig. 3. (The corresponding diagram for the Bethe lattice is given in Fig. 2 of ref. 7.) The line of critical points for this case is plotted for each of the three lattices in Fig. 4.

In the above case, for which $s = 1$, hydrogen bonding between A and B molecular ends promotes mixing at low temperatures. Phase separation

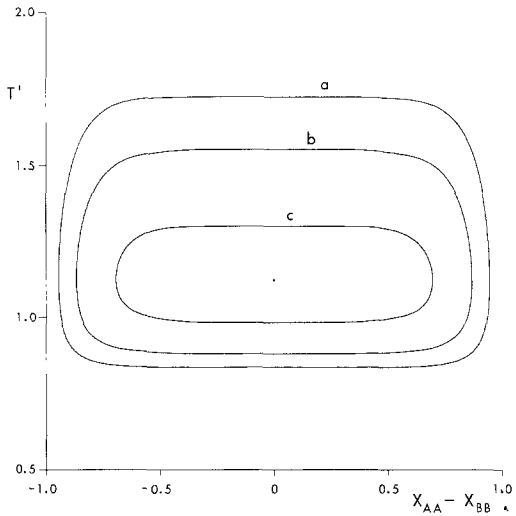

Fig. 2. Closed-loop phase diagrams for the model on the honeycomb lattice for the case $s = 1$, $u = 0$, and $q_A = q_B = 6$. The value of X_{AB} on each of the loops is given as (a) $X_{AB} = 0.00$, (b) $X_{AB} = 0.02$, and (c) $X_{AB} = 0.04$. The closed loops shrink to a double critical point at $T'_D = 4/\ln 35 = 1.125...$ and $X^D_{AB} = 0.045667....$

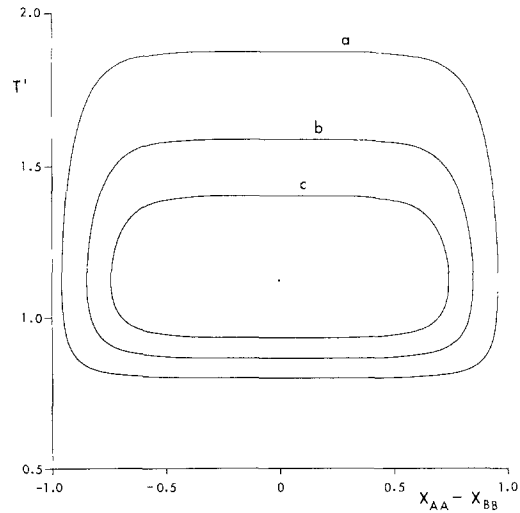

Fig. 3. Closed-loop phase diagrams for the model on the square lattice for the case $s = 1$, $u = 0$, and $q_A = q_B = 6$. The value of X_{AB} on each of the loops is given as (a) $X_{AB} = 0.00$, (b) $X_{AB} = 0.04$, and (c) $X_{AB} = 0.06$. The closed loops shrink to a double critical point at $T'_D = 4/\ln 35 = 1.125...$ and $X^D_{AB} = 0.074154....$

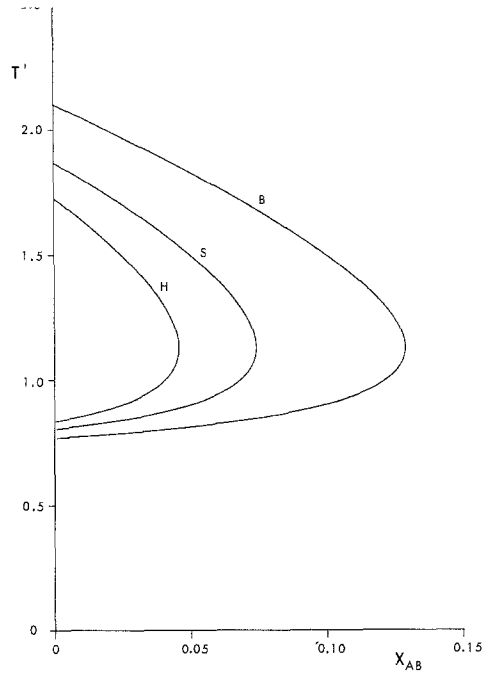

Fig. 4. The line of critical solution points for the model on the Bethe lattice (B), on the square lattice (S), and on the honeycomb lattice (H) for the case $s = 1$, $u = 0$, and $q_A = q_B = 6$. There is a double critical point at $T'_D = 4/\ln 35 = 1.125...$ which corresponds to a maximum of X^c_{AB}.

into AA-rich and BB-rich phases occurs at moderate temperatures due to the large number of states corresponding to repulsions between A and B ends. (These states represent molecular orientations.) As the mole fraction of AB molecules increases, mixing is enhanced and the closed loops shrink to a point at a double critical point.

We wish to also consider the possibility of a low-temperature miscibility gap which has an upper critical point below the temperature of the lower critical point of the closed loop.[3,4] At a certain value of X_{AB}, these two critical points can coalesce into a double critical point. In order to have a miscibility gap at low temperatures, R must remain sufficiently large as $T' \to 0$. Equation (5) yields, as $T' \to 0$,

$$e^{-2R} \to \frac{1}{q_B} e^{(2s-u)/T'} \tag{11}$$

Hence $u > 2s$ is a necessary condition for a miscibility gap to occur at low temperatures. This condition implies that a hydrogen bond between two

type A ends must be energetically stronger than a hydrogen bond between a type A and a type B end, the latter type of bond promoting mixing at low temperatures.

In order to have mixing at moderate temperatures, above the miscibility gap and below the closed loop, the hydrogen bonding between A and B molecular ends must be more prevelant than the hydrogen bonding between two type A molecular ends. This can be accomplished entropically if $q_A \gg q_B$. Using these qualitative guides, it is easy to locate cases of the model which contain a low-temperature miscibility gap in addition to a closed loop.

We have calculated the coexistence curves for several values of X_{AB} for the model on the Bethe and honeycomb lattices for the case $s=1$, $u=2.01$, $q_A=60$, and $q_B=3$. The phase diagram for this case on the Bethe lattice is illustrated in Fig. 5, and the phase diagram for this case on the honeycomb lattice is illustrated in Fig. 6. The line of critical points for this case for all three lattices is illustrated in Fig. 7. The two types of double critical points are present in this case of the model on each of the three lattices.

In Section 4 we calculate the nature of the critical exponent β near critical and double critical points for coexistence curves in $X_{AA}-X_{BB}$, T' planes which have constant values of X_{AB}.

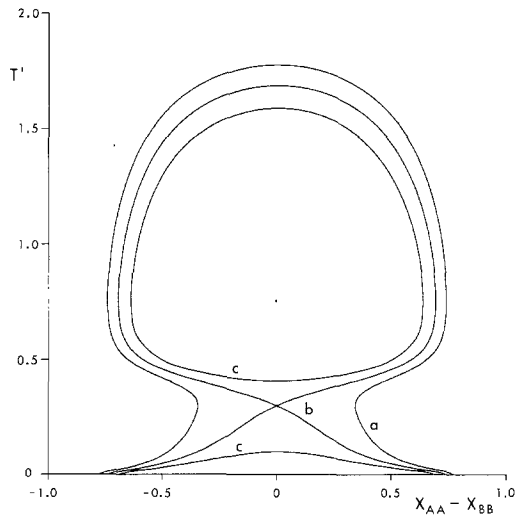

Fig. 5. Closed-loop phase diagrams for the model on the Bethe lattice for the case $s=1$, $u=2.01$, $q_A=60$, and $q_B=3$. The value of X_{AB} on each of the loops is given as (a) $X_{AB}=0.12$, (b) $X_{AB}=X_{AB}^{D}=0.13462$, and (c) $X_{AB}=0.15$. A double critical point occurs in case (b) at $T_D'=0.30059$. The closed loops shrink to a double critical point at $X_{AB}^{D}=0.22857$ and $T_D'=0.75533$.

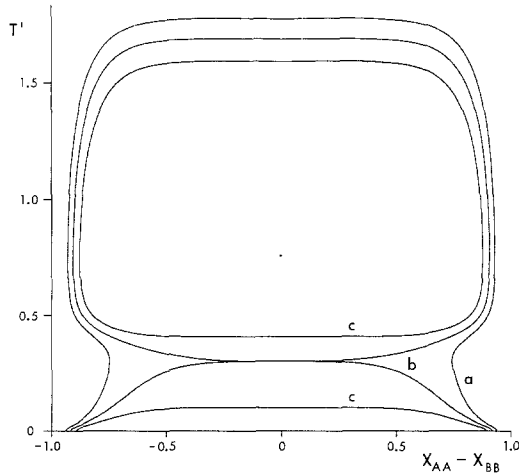

Fig. 6. Closed-loop phase diagrams for the model on the honeycomb lattice for the case $s=1$, $u=2.01$, $q_A=60$, and $q_B=3$. The value of X_{AB} on each of the loops is given as (a) $X_{AB}=0.04$, (b) $X_{AB}=X_{AB}^{D}=0.049657$, and (c) $X_{AB}=0.06$. A double critical point occurs in case (b) at $T_D'=0.30059$. The closed loops shrink to a double critical point at $X_{AB}^{D}=0.10588$ and $T_D'=0.75533$.

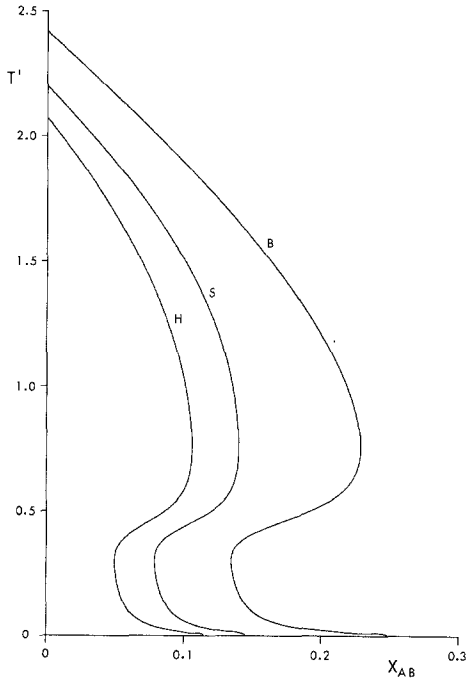

Fig. 7. The line of critical solution points for the model on the Bethe lattice (B), on the square lattice (S), and on the honeycomb lattice (H) for the case $s=1$, $u=2.01$, $q_A=60$, and $q_B=3$. There are two double critical points at temperatures $T_D'=0.75533$ and $T_D'=0.30059$, which correspond to a local maximum and a local minimum of X_{AB}^{c}, respectively.

4. DOUBLING OF THE CRITICAL EXPONENT β

As mentioned by several authors,[1-11] the critical exponents double near a double critical point. We wish to calculate explicitly the nature of the doubling of β near double critical points in the present model. In particular, for the model on the Bethe and honeycomb lattices, we shall calculate the behavior of the order parameter $|X_{AA}-X_{BB}|$ along coexistence curves near critical and double critical points in $X_{AA}-X_{BB}$, T' planes at constant X_{AB}.

The models on both the Bethe and the honeycomb lattices are related to an Ising model on these lattices with a coupling constant K. The constant L is related to K and R as[12]

$$e^{-2L}=\frac{e^{-2K}(e^{4R}+1)-2}{e^{4R}+1-2e^{-2K}} \tag{12}$$

Equation (12) can be substituted into the closed-form expressions for I_Δ and σ_Δ given in the Appendix to yield I_Δ and σ_Δ as functions of $y=\exp(-4R)$ and $z=\exp(-2K)$. From the expression for I_Δ, we find that near a critical point

$$I_\Delta \sim A_\Delta (z_c-z)^\beta \tag{13}$$

where $\beta=1/2$ for the Bethe lattice and $\beta=1/8$ for the honeycomb lattice.

Since $X_{AB}=(1-\sigma_\Delta)/2$, the expression for σ_Δ as a function of y and z can be used to obtain functional relationships between $\Delta y=y_c-y$ and $\Delta z=z_c-z$ near critical points along coexistence curves in planes of constant X_{AB}. We obtain

$$\begin{aligned} &\Delta y \sim B_1\,\Delta z && \text{Bethe} \\ &\Delta y \sim B_2\,\Delta z \ln \Delta z && \text{honeycomb} \end{aligned} \tag{14}$$

The logarithmic behavior is common for two-dimensional lattices[15] and results here as the limiting form of the elliptic integral which occurs in the expression for σ_Δ. Combining Eqs. (13) and (14), we obtain

$$\begin{aligned} &I_\Delta \sim B_3\,\Delta y^\beta && \text{Bethe} \\ &I_\Delta \sim B_4\left(\frac{\Delta y}{-\ln I_\Delta}\right)^\beta && \text{honeycomb} \end{aligned} \tag{15}$$

Expanding Eq. (5) near a critical point, we obtain

$$\Delta y \sim a_c\,\Delta'_T + b_c(\Delta'_T)^2 \tag{16}$$

where $\Delta'_T = T'_c - T'$. Since two values of T' give the same value of R near a double critical point and coincide at T'_D at a double critical point, then R is an extremum at a double critical point. Thus the constant a_c in Eq. (16) vanishes at a double critical point. With this behavior of a_c in mind, we substitute Eq. (16) into Eq. (15) to obtain I_Δ near a normal critical point as

$$\begin{aligned} I_\Delta &\sim B_5 \,|T' - T'_c|^\beta && \text{Bethe} \\ I_\Delta &\sim B_6 \left(\frac{|T' - T'_c|}{-\ln I_\Delta} \right)^\beta && \text{honeycomb} \end{aligned} \tag{17}$$

and I_Δ near a double critical point as

$$\begin{aligned} I_\Delta &\sim B_7 \,|T' - T'_D|^{2\beta} && \text{Bethe} \\ I_\Delta &\sim B_8 \left(\frac{|T' - T'_D|}{(-\ln I_\Delta)^{1/2}} \right)^{2\beta} && \text{honeycomb} \end{aligned} \tag{18}$$

Expressions (17) are satisfied along coexistence curves in constant-X_{AB} planes near all normal critical points illustrated in Figs. 2, 3, 5, and 6. Expressions (18) are satisfied near the double critical points in Figs. 5 and 6 which join the closed loop to the low-temperature miscibility gap.

Expressions (17) were found to hold in constant-X_{AB} planes near to but not including the double critical point which occurs when the closed loop shrinks to a point. This behavior occurs since a critical point on each closed loop, no matter how small the loop, is not a true double critical point. Hence a_c of Eq. (16), although small, is nonzero. Very near the critical point, where $a_c \gg b_c \Delta_{T'}$, the behavior of (17) is thus observed. It is possible there could be a range of T' relatively near T'_c at which $a_c \ll b_c \Delta_{T'}$, and the behavior of (18) would result there. As $X_{AB} \to X^D_{AB}$, the range of T' at which (18) holds would grow. However, our calculations indicate that the loop shrinks in size so fast that this range of T' is never realized.

5. THE CRITICAL LINE NEAR A DOUBLE CRITICAL POINT

In this section we calculate the nature of the critical line in the neighborhood of the double critical point which occurs when the closed-loop phase diagram shrinks to a point. For this analysis, we consider only the case $u = 0$. For each of the three lattices, the critical line for the case $u = 0$, $s = 1$, and $q_A = q_B = 6$ is plotted in Fig. 4. Since, as mentioned in Section 4, R_c is an extremum at the double critical point, then Eq. (5)

can be used to calculate the lattice-independent temperature of the double critical point as

$$T'_D = 2(s+1)/\ln[(1-\sigma_{AB})/(s\sigma_{AB})] \tag{19}$$

For the model on each of the three lattices, the relationships between R_c and L_c given by Eq. (9) can be used to convert previously given[12–14] expressions for X^c_{AB} as functions of R_c and L_c into expressions depending only on the variable $y_c = \exp(-4R_c)$. This yields the following expressions for the Bethe lattice

$$X^c_{AB} = (1-5y_c)/(4-4y_c) \tag{20}$$

for the honeycomb lattice

$$X^c_{AB} = 1/2 - 2(1+3y_c+6y_c^2)/[3^{3/2}(1+3y_c)(1-y_c)] \tag{21}$$

and for the square lattice

$$X^c_{AB} = \frac{-(\tau_c-1)^2}{\tau_c(2-\tau_c)} + \frac{2}{\pi(2-\tau_c)}\left(\frac{\tau_c-1}{\tau_c+1}\right)^{1/2} \cos^{-1}\left(\frac{1}{\tau_c}\right) \tag{22}$$

where $\tau_c = \sqrt{2}\,(1-y_c)/(1+y_c)$.

In order to elucidate the behavior of the critical line in the neighborhood of the double critical point, we note that, letting $\Delta_T = (T_c - T_D)/T_D$, we can use Eq. (5) with $u=0$ to obtain the expansion

$$y_c \sim y_D[1+\alpha_0 \Delta_T^2(1-2\alpha_1 \Delta_T)] \tag{23}$$

where, for $u=0$,

$$\begin{aligned} \alpha_0 &= 4s/(T'_D)^2 \\ \alpha_1 &= 1+(s-1)/(3T'_D) \\ y_D &= (s+1)^2\,\sigma_{AB}^2[(1-\sigma_{AB})/(s\sigma_{AB})]^{2s/(s+1)} \end{aligned} \tag{24}$$

and T'_D is given by Eq. (19). Substitution of Eq. (23) into Eqs. (20)–(22) yields

$$(X^D_{AB} - X_{AB})^{1/2} \sim (\alpha_0 \beta_D)^{1/2}\,|\Delta_T|\,(1-\alpha_1 \Delta_T) \tag{25}$$

where β_D is a lattice-dependent function of y_D. We obtain for the Bethe lattice

$$\beta_D = y_D(1-y_D)^{-2} \tag{26}$$

for the honeycomb lattice

$$\beta_D = 3^{-3/2} y_D [5(1-y_D)^{-2} - 3(1+3y_D)^{-2}] \tag{27}$$

and for the square lattice

$$\beta_D = \frac{2-\tau_D^2}{\sqrt{2}\,\tau_D^2(2-\tau_D)^2(1+\tau_D)} \times \left[1-\tau_D^2 + \frac{\tau_D(2-\tau_D)}{\pi} + \frac{\tau_D^2(\tau_D^2-\tau_D+1)\cos^{-1}(1/\tau_D)}{\pi(\tau_D^2-1)^{1/2}}\right] \tag{28}$$

Expanding Δ_T as a series in $(X_{AB}^D - X_{AB})^{1/2}$ and then adding and subtracting the equations which result when T_U and T_L are substituted for T_c in Δ_T yields the expressions given in Eq. (1), where the constants A and B are given as

$$\begin{aligned} A &= (\alpha_0 \beta_D)^{-1/2} \\ B &= \alpha_1 A^2 \end{aligned} \tag{29}$$

Equation (29) contains as a special case the expression for A previously calculated[7] for the model on the Bethe lattice for the case $u=0$ and $s=1$. For the case $u=0$, $s=1$, and $q_A = q_B = 6$, Eq. (29) yields $B=A^2$, $A=1.527$ for the Bethe lattice, $A=1.824$ for the honeycomb lattice, and $A=1.698$ for the square lattice. For the case $u=0$, $s=5$ and $q_A = q_B = 60$, Eq. (29) yields $B=1.731A^2$, $A=0.8543$ for the Bethe lattice, and $A=0.9057$ for the square lattice. The honeycomb lattice has no closed loops for this latter case, for $R(T'_D)=0.457$ is less than min R_c for the honeycomb lattice as given by Eq. (10).

Hence, for all values of the parameters for which closed-loop phase diagrams occur, we have shown that the critical line for the model on the Bethe, honeycomb, and square lattices exhibits the same type of behavior in the neighborhood of the double critical point, which occurs as the limit of closed-loop diagrams, as has been found experimentally for some systems.[8-10] As is evident from Eqs. (23) and (25), the type of behavior given by Eq. (1) is also exhibited by the model on *any* lattice for which X_{AB}^c is an analytic function of y_c. The lattice-dependent constant β_D is then given as $\beta_D = -y_D\, dX_{AB}^c/dy_c|_{y_D}$. Consequently, Eq. (1) probably holds for the model on three-dimensional lattices as well.

APPENDIX. EXACT EXPRESSIONS FOR I_Λ AND σ_Λ

The following are exact expressions for I_Λ and σ_Λ for the Bethe, honeycomb, and square lattices. We denote Λ for the Bethe lattice as Λ_∞.

The Λ for the honeycomb lattice is the 3–12 lattice, and Λ for the square lattice is the 4–8 lattice. Although used in ref. 13, the formula for $I_{4\text{-}8}$ was not proved to be exact until later.[16,17]

For the model on the Bethe lattice,[14] where $z = \exp(-2K)$,

$$I_{\Lambda_\infty} = \frac{(e^{4R}+3)^{1/2}\,(e^{4R}-1)^{1/2}}{(e^{4R}+1+2e^{-2L})}\,\frac{1}{1-2z}\left(\frac{1-3z}{1+z}\right)^{1/2}$$

$$\sigma_{\Lambda_\infty} = \coth 2L - \frac{1}{\sinh 2L}\left(\frac{z}{1-2z}\right)$$

For the model on the honeycomb lattice,[12]

$$I_{3\text{-}12} = \frac{(e^{4R}+3)^{1/2}\,(e^{4R}-1)^{1/2}\,(1-\kappa^2)^{1/8}}{e^{4R}+1+2e^{-2L}}$$

$$\sigma_{3\text{-}12} = [2\eta \mathbf{K}(\kappa)\sinh 2K - \cosh 2K]/(3\sinh 2L) + \coth 2L$$

where

$$\kappa^2 = 16z^3(1+z^3)(1-z)^{-3}\,(1-z^2)^{-3}$$

$$\eta = (1-z^4)(z^2-4z+1)/[\pi\,|1-z^2|\,(1-z)^4]$$

$$\mathbf{K}(k) = \int_0^{\pi/2} (1-k^2\sin^2\theta)^{-1/2}\,d\theta$$

For the model on the square lattice, $I_{4\text{-}8}$ is given as[13]

$$I_{4\text{-}8} = [1+e^{-2L}(\cosh 2R)^{-2}]^{-1/2}\,(1-\kappa_S^2)^{1/8}$$

where

$$\kappa_S^2 = \{[2t_1t_2(1-t_1^2)]^4 + [(1+2t_1^2t_2^2+t_1^4)^2 - 16t_1^4t_2^2] \times (1-2t_1^2t_2^2+t_1^4)^2\}[2t_1t_2(1+t_1^2)]^{-4}$$

and $t_1 = \tanh R$ and $t_2 = \tanh L$.

For the square lattice, letting

$$\alpha = 4\cosh^2 2R\sinh^2 2R\sinh^2 2L + 4(\cosh^2 2R + \cosh 2L)^2$$

$$\beta = -2\sinh^2 2R\sinh 2L\,(\cosh^2 2R + \cosh 2L)$$

$$\delta = -\sinh^2 2R\sinh^2 2L$$

$\sigma_{4\text{-}8}$ is given as[13]

$$\sigma_{4\text{-}8} = \frac{1}{4}\left[\frac{\partial I}{\partial\alpha}\frac{\partial\alpha}{\partial L} + \frac{\partial I}{\partial\beta}\frac{\partial\beta}{\partial L} + \frac{\partial I}{\partial\delta}\frac{\partial\delta}{\partial L}\right]\Bigg|_R$$

where I is an integral defined in ref. 13, and

$$\frac{\partial I}{\partial \alpha} = \frac{2\mathbf{K}(k)}{\pi(\alpha - 4\delta)}$$

$$\frac{\partial I}{\partial \beta} = \frac{-4(\alpha + 2\beta)\,\mathbf{K}(k) + 4(\alpha + 4\beta + 4\delta)\,\Pi_1(v, k)}{\pi(\alpha - 4\delta)(\beta + 2\delta)}$$

$$\frac{\partial I}{\partial \delta} = \frac{2(\alpha\beta - 2\alpha\delta + 4\beta^2)\,\mathbf{K}(k) - 4\beta(\alpha + 4\beta + 4\delta)\,\Pi_1(v, k)}{\pi\delta(\alpha - 4\delta)(\beta + 2\delta)} + \frac{1}{\delta}$$

$$\Pi_1(v, k) = \int_0^{\pi/2} (1 + v \sin^2\theta)^{-1} (1 - k^2 \sin^2\theta)^{-1/2}\, d\theta$$

$$k^2 = 16(\beta^2 - \alpha\delta)/(\alpha - 4\delta)^2$$

$$v = 4(\beta + 2\delta)/(\alpha - 4\delta)$$

ACKNOWLEDGMENT

This research was supported by the Robert A. Welch Foundation, grant P-446.

REFERENCES

1. J. T. Bartis and C. K. Hall, *Physica* **78**:1 (1974).
2. J. C. Wheeler, *Annu. Rev. Phys. Chem.* **28**:411 (1977).
3. J. C. Wheeler and G. R. Anderson, *J. Chem. Phys.* **73**:5778 (1980).
4. R. E. Goldstein and J. S. Walker, *J. Chem. Phys.* **78**:1492 (1983).
5. J. S. Walker and C. A. Vause, *J. Chem. Phys.* **79**:2660 (1983).
6. R. E. Goldstein, *J. Chem. Phys.* **79**:4439 (1983).
7. D. A. Huckaby and M. Shinmi, *J. Chem. Phys.* **90**:5675 (1989).
8. R. G. Johnston, N. A. Clark, P. Wiltzius, and D. S. Cannell, *Phys. Rev. Lett.* **54**:49 (1985).
9. C. M. Sorensen and G. A. Larsen, *J. Chem. Phys.* **83**:1835 (1985).
10. A. Kumar, S. Guha, and E. S. R. Gopal, *Phys. Lett. A* **123**:489 (1987).
11. R. B. Griffiths and J. C. Wheeler, *Phys. Rev. A* **2**:1047 (1970).
12. D. A. Huckaby and M. Shinmi, *J. Stat. Phys.* **45**:135 (1986).
13. M. Shinmi and D. A. Huckaby, *J. Phys. A* **20**:L465 (1987).
14. D. A. Huckaby, M. Shinmi, and V. A. Belfi, *Physica A* **154**:521 (1989).
15. B. Widom, *J. Chem. Phys.* **46**:3324 (1967).
16. R. J. Baxter and T. C. Choy, *J. Phys. A* **21**:2143 (1988).
17. K. Y. Lin, *Phys. Lett. A* **128**:35 (1988).